Supporting Information for

Controllable Growth of High-Quality Metal Oxide/Conducting Polymer Hierarchical Nanoarrays with Outstanding Electrochromic Properties and Solar-Heat Shielding Ability

Dongyun Ma,[a,d] Guoying Shi,[c] Hongzhi Wang,*[a] Qinghong Zhang,[b] and Yaogang Li*[b]

[a] State Key Laboratory for Modification of Chemical Fibers and Polymer Materials, College of Materials Science and Engineering, Donghua University, Shanghai 201620, P. R. China. Fax: +86-021-67792855; Tel: +86-021-67792881; E-mail: wanghz@dhu.edu.cn

[b] Engineering Research Center of Advanced Glasses Manufacturing Technology, Ministry of Education, College of Materials Science and Engineering, Donghua University, Shanghai 201620, P. R. China. Fax: +86-021-67792855; Tel: +86-021-67792526; E-mail: yaogang_li@dhu.edu.cn

[c] College of Chemistry, Chemical Engineering and Biotechnology, Donghua University, Shanghai 201620, China.

[d] School of Materials Science and Engineering, Shanghai University, Shanghai 200444, People's Republic of China.

For the preparation of the organic part of hybrid materials, electrochemical polymerization is indeed an attractive method because the morphologies of polymers can be controlled through simple adjustment of the parameters of the synthetic procedure. Fig. S1 shows the FESEM images of PANI films prepared using different electropolymerization procedures. It can be seen that PANI films with amorphous morphologies were obtained under both potentio- and galvanostatic procedures, while the crystalline PANI nanorod-like films were grown using a potential cycling protocol. For the amorphous PANI, polymeric macromolecules are too big to penetrate into the pores of a nanostructured metal oxide matrix (especially if it is already partially loaded), resulting in insufficient pore filling. The net result is that the organic component resides dominantly at the upper areas of the nanoporous metal oxides.
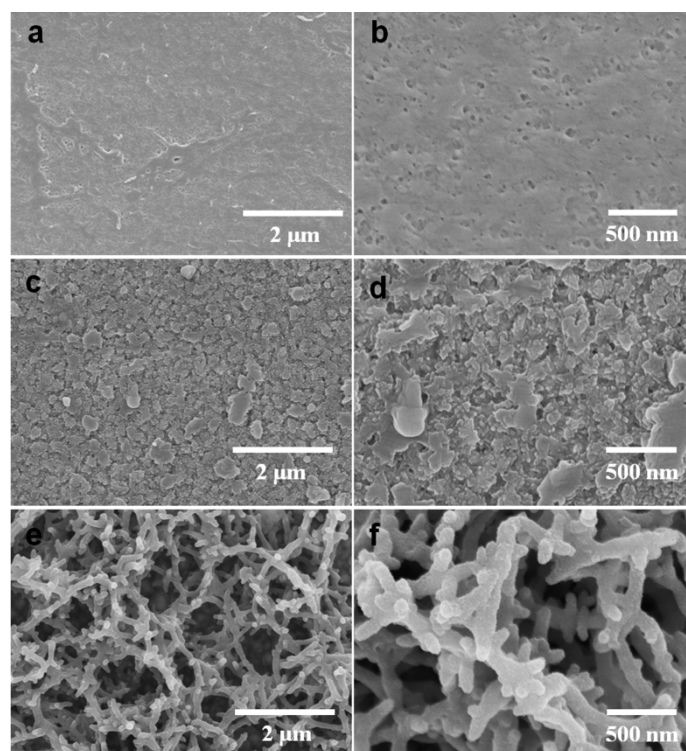
Fig. S1 FESEM images of PANI films prepared using (a, b) potentiostatic procedure at 1.2 V for 2 min, (c, d) galvanostatic procedure with current density of 0.5 mA/cm^2 for 10 min and (e, f) potentiodynamic cycle at a sweep rate of 100 mV/s for 100 cycles between -0.6 and 1.2 V.

Fig. S2 shows the XRD patterns of the porous NiO films prepared in the reaction

solution containing different structure-directing agent and solvent. From the XRD patterns, it was confirmed that all the diffraction peaks of the samples were indexed to the cubic NiO phase (JCPDS no. 04-0835).
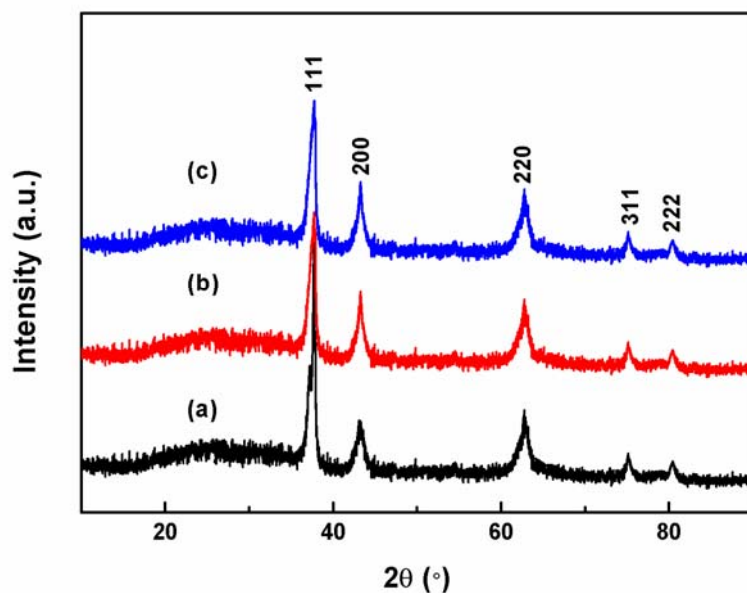
Fig. S2 XRD patterns of porous NiO films synthesized with (a) addition of 0.6 g urea, where water was used as solvent, (b) addition of 0.6 g urea, where ethanol was used as solvent and (c) addition of 0.3 g $K_2S_2O_8$ and 3 mL NH_3H_2O, where water was used as solvent,.
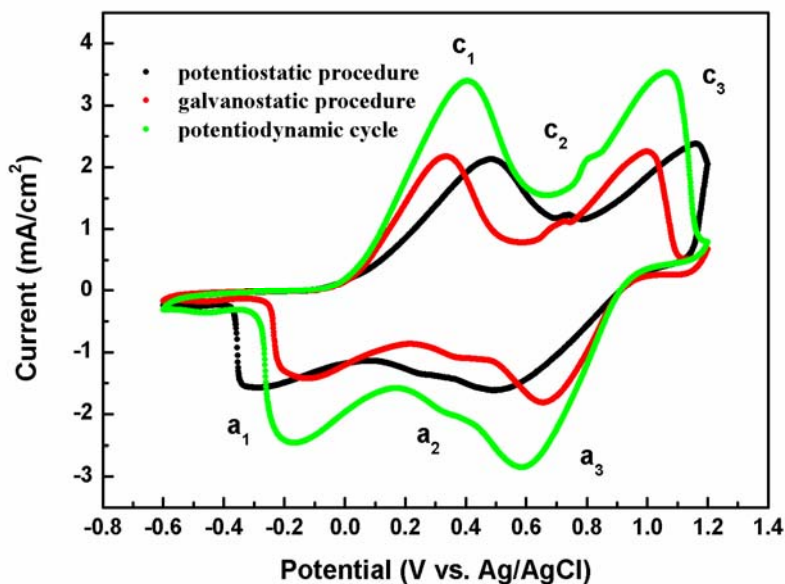
Fig. S3 Cyclic voltammetry curves of PANI films deposited by potentiostatic, galvanostatic procedures and potentiodynamic cycle.

Fig. S3 shows the cyclic voltammetry curves of PANI films deposited by potentiostatic, galvanostatic procedures and potentiodynamic cycle, respectively, which have three typical redox peaks (c_1/a_1, c_2/a_2 and c_3/a_3). The redox couples c_1/a_1 and c_3/a_3 correspond to the change between leucoemeraldine salt (LS) and emeraldine salt (ES), emeraldine salt (ES) and pernigraniline salt (PS) of PANI with anion doping/dedoping processes, respectively. The redox couple c_2/a_2 can be ascribed to hydrolysis products of PANI due to over-oxidation at comparatively high potential.
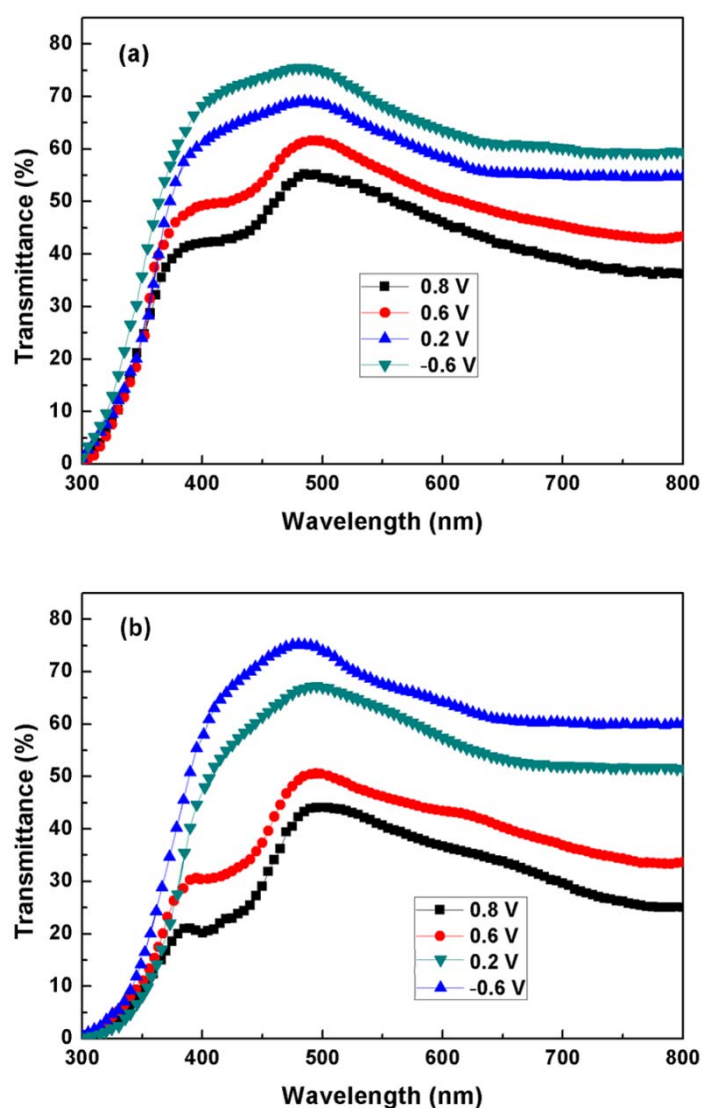
Fig. S4 Transmittance spectra of PANI films under different voltages: (a) PANI films prepared by potentiostatic procedure, (b) PANI films prepared by galvanostatic procedure.
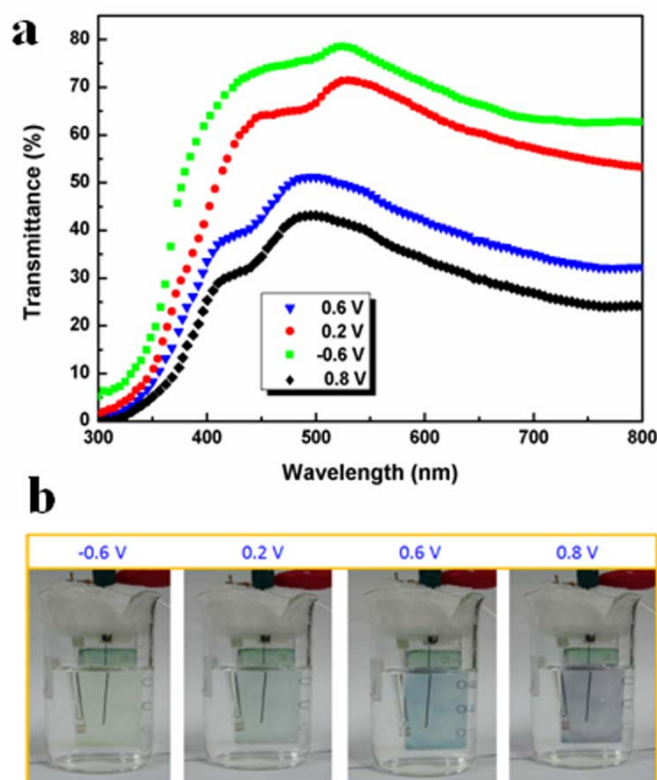
Fig. S5 (a) Transmittance spectra of PANI films prepared by potentiodynamic cycle under different voltages, (b) the corresponding digital photos of PANI films under different voltages.

The as-prepared single PANI films show rich reversible color changes ranging from yellow, green, and blue to purple under different applied potentials (Fig. S5b). However, the hybrid WO$_3$/PANI or NiO/PANI films show more obvious color changes under different voltages (Fig. 5b and Fig. 6d in the article) than the single PANI films because the porous oxides provide not only a stable mechanical support for the active PANI but also a template for homogeneous coverage of PANI, leading to a synergistic electrochromism effect. The corresponding optical changes of the PANI films are recorded by the transmittance spectra (as shown in Fig. S4 and Fig. S5b). According to the definitions for the optical modulation in the article, the maximum values of 22%, 26% and 32% are reached between -0.6 and 0.8 V for PANI films deposited by potentiostatic, galvanostatic procedures and potentiodynamic cycle, respectively.

The switching times and coloration efficiency for the PANI films prepared by potentiodynamic cycle were measured and shown in Fig. S6. The response times

under the voltages of -0.6 and 0.8 V are found to be 300 and 500 ms, respectively, faster than those of the WO_3/PANI films (500 and 800 ms, respectively). The poor conductivity of inorganic container (WO_3 is insulating, especially at positive potential) is responsible for the slow switching speed of the WO_3/PANI films. The calculated CE value of the PANI films is 49.2 cm^2 C^{-1}, which is much lower than those of both the WO_3/PANI and NiO/PANI films.
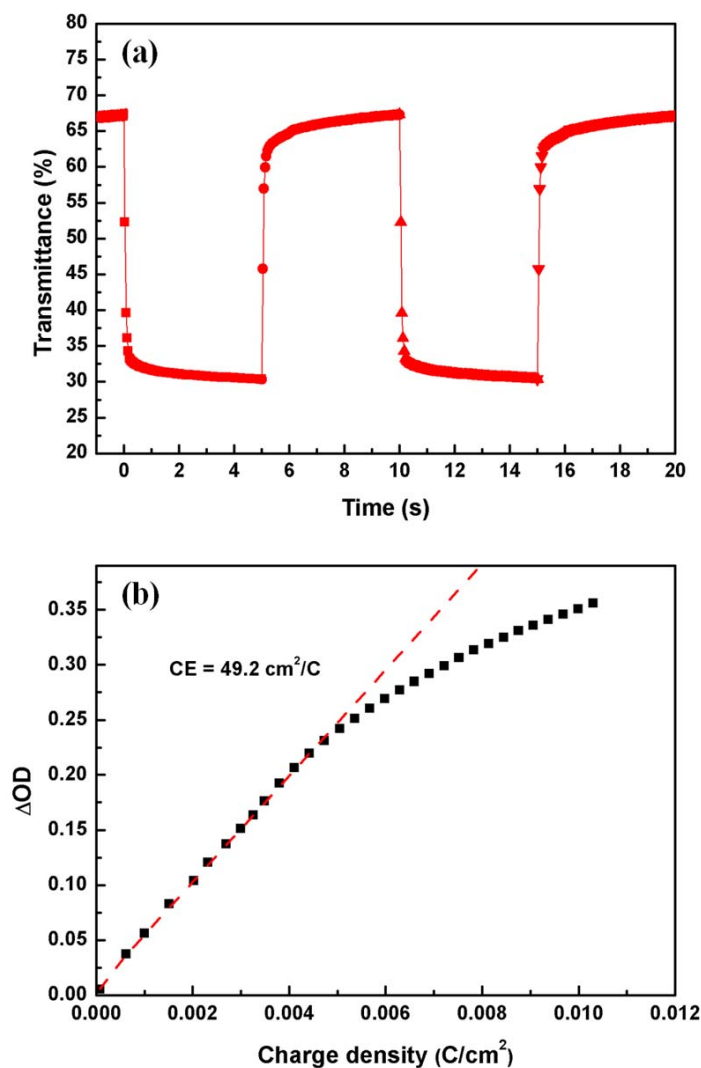
Fig. S6 (a) Switching time characteristics measured at 632.8 nm between -0.6 and 0.8 V and (b) ΔOD variation with respect to the charge density for the PANI films prepared by potentiodynamic cycle.
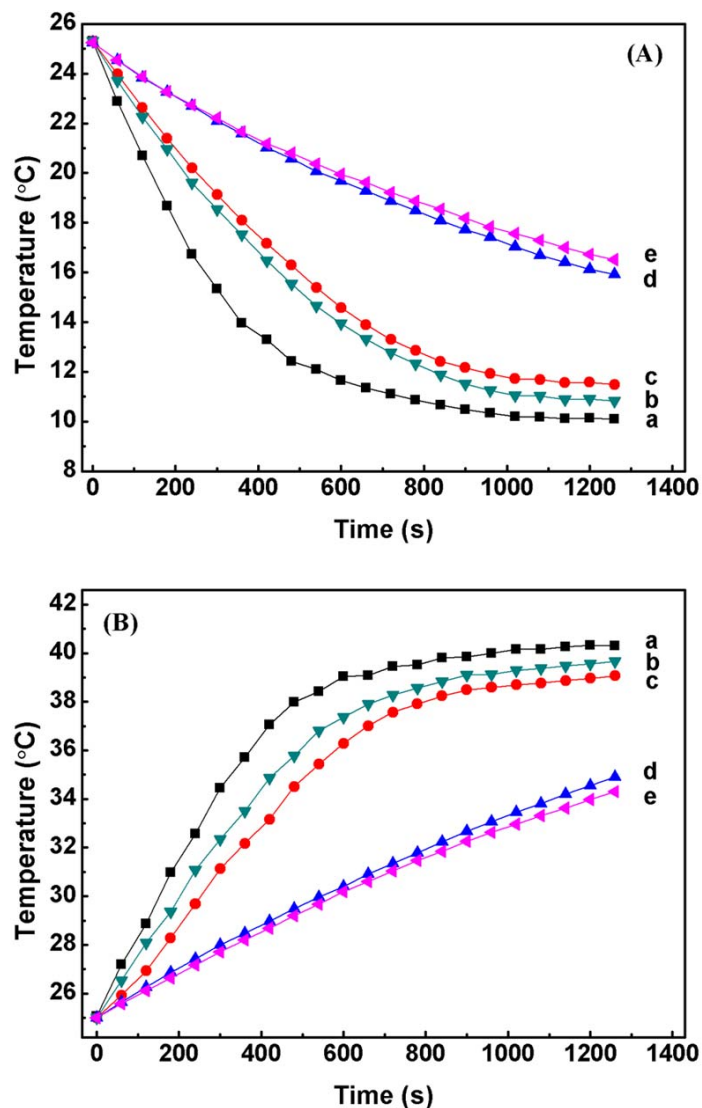
Fig. S7 (A) Temperature dependence on time for NiO/PANI coated FTO glass with the temperature of thermostatic chamber fixed at 10 °C, a: blank FTO glass, b and d: NiO/PANI-2/FTO glass after applying potentials of -0.6 V and 1.2 V, respectively, c and e: NiO/PANI-1/FTO glass after applying potentials of -0.6 V and 1.2 V, respectively; (B) Temperature dependence on time for NiO/PANI coated FTO glass with the temperature of thermostatic chamber fixed at 40 °C, a: blank FTO glass, b and d: NiO/PANI-2/FTO glass after applying potentials of -0.6 V and 1.2 V, respectively, c and e: NiO/PANI-1/FTO glass after applying potentials of -0.6 V and 1.2 V, respectively.
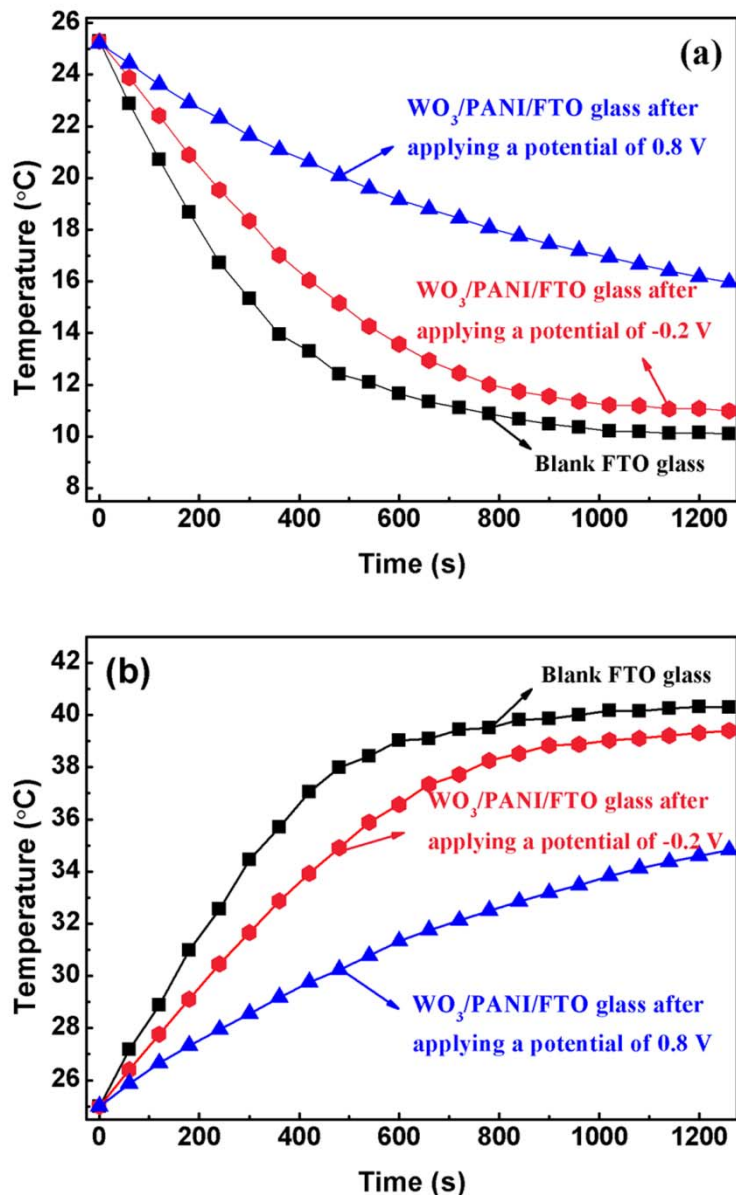
Fig. S8 (a) and (b) temperature dependence on time for WO$_3$/PANI coated FTO glass with the temperature of thermostatic chamber fixed at 10 and 40 °C, respectively.

In this work, we have constructed a model house (as mentioned in the article) to evaluate the solar-heat shielding ability of WO$_3$/PANI and NiO/PANI hybrids coated FTO glass. Fig. S7 and S8 show temperature dependence on time for NiO/PANI-1, NiO/PANI-2 and WO$_3$/PANI coated FTO glass with the temperature of thermostatic chamber fixed at 10 and 40 °C, respectively. The values calculated from Fig. S7 indicate that the application of the NiO/PANI-1 and NiO/PANI-2 coated FTO glass causes temperature differences of about 4.7 and 4.2 °C (when the outer room (thermostatic chamber) temperature fix at 10 °C) compared with the blank FTO glass,

respectively. In another case (when the outer room temperature fix at 40 °C), temperature reduction of about 4.6 and 4.3 °C are achieved for the NiO/PANI-1 and NiO/PANI-2 coated FTO glass, respectively. The values calculated from Fig. S8 indicate that the application of the WO$_3$/PANI coated FTO glass causes a temperature difference of about 4.4 °C (when the outer room temperature fix at 10 °C) compared with the blank FTO glass. In another case (when the outer room temperature fix at 40 °C), a temperature reduction of about 4.2 °C is achieved for the WO$_3$/PANI coated FTO glass.
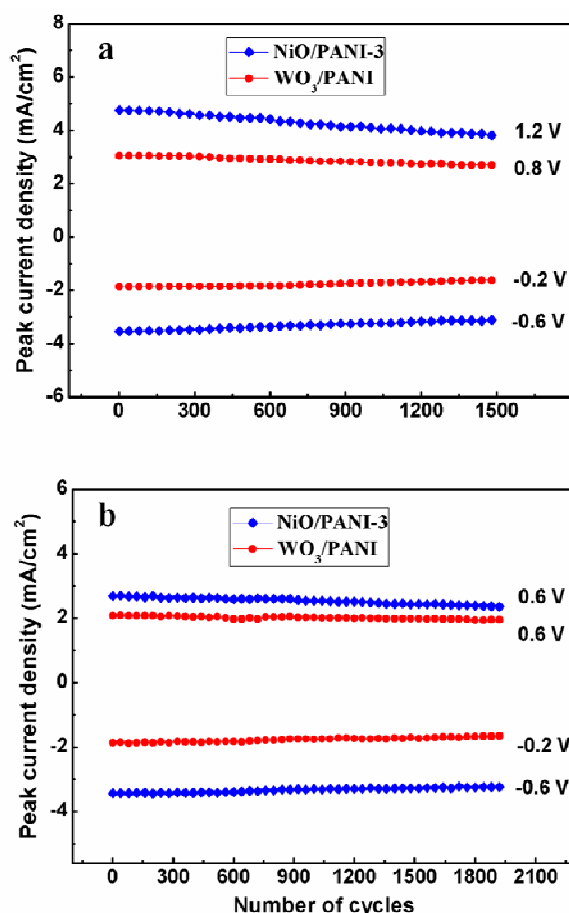
Fig. S9 Peak current evolution of the WO$_3$/PANI and NiO/PANI-3 films during the step chronoamperometric cycles under different potentials.

The cycle stability of the WO$_3$/PANI and NiO/PANI-3 films is characterized by chronoamperometry using the corresponding square potentials mentioned in the manuscript. The evolution of corresponding redox peak currents is presented in Fig. S9. For WO$_3$/PANI films, the degradations of the peak currents at 0.8 and -0.2 V after 1500 cycles are 13.5% and 12.7%, respectively. For NiO/PANI-3 films, the degradations of the peak currents at 1.2 and -0.6 V after 1500 cycles are 21% and

13.1%, respectively. It is confirmed that the PANI is not stable as a result of benzoquinone formation by hydrolysis during cycling, especially under a potential higher than 0.7 V. We therefore have also investigated the cycling stability of EC devices based on WO$_3$/PANI and NiO/PANI films at a low oxidation potential of 0.6 V (as shown in the Fig. S9b). The degradations of the peak currents at 0.6 V after 2000 cycles for the WO$_3$/PANI and NiO/PANI-3 films based on EC devices are 6% and 9.3%, respectively. Obviously, the cycle stability of the EC devices assembled by WO$_3$/PANI and NiO/PANI-3 films is highly enhanced when a low oxidation potential was applied.